

This paper is published as part of a *Dalton Transactions* themed issue entitled:

Polyoxometalates

Guest Editors: De-Liang Long and Leroy Cronin

Published in issue 33, 2012 of *Dalton Transactions*

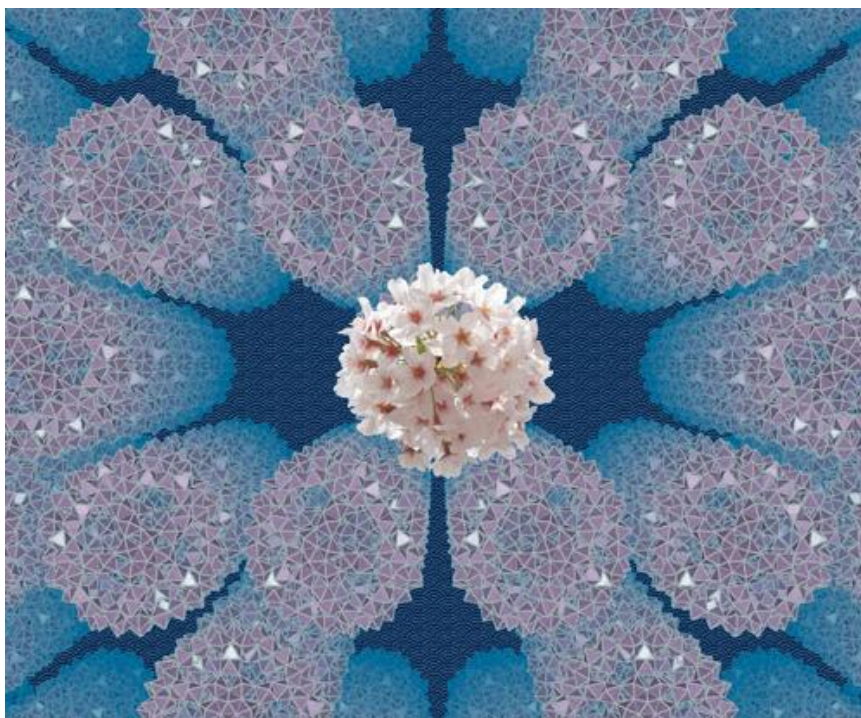


Image reproduced with permission of Tomoji Ozeki

Articles published in this issue include:

[Polyoxometalates as efficient catalysts for transformations of cellulose into platform chemicals](#)

Weiping Deng, Qinghong Zhang and Ye Wang
Dalton Trans., 2012, DOI: 10.1039/C2DT30637A

[Surfactant-encapsulated polyoxometalate building blocks: controlled assembly and their catalytic properties](#)

Amjad Nisar and Xun Wang
Dalton Trans., 2012, DOI: 10.1039/C2DT30470H

[A dodecanuclear Zn cluster sandwiched by polyoxometalate ligands](#)

Guibo Zhu, Yurii V. Geletii, Chongchao Zhao, Djamaladdin G. Musaev, Jie Song and Craig L. Hill
Dalton Trans., 2012, DOI: 10.1039/C2DT30733B

Visit the *Dalton Transactions* website for more cutting-edge inorganic research
www.rsc.org/dalton

Cite this: *Dalton Trans.*, 2012, **41**, 9979

www.rsc.org/dalton

PAPER

Structural and dynamical aspects of alkylammonium salts of a silicodectungstate as heterogeneous epoxidation catalysts†

Sayaka Uchida,‡ Keigo Kamata, Yoshiyuki Ogasawara, Megumi Fujita and Noritaka Mizuno*

Received 1st March 2012, Accepted 26th March 2012

DOI: 10.1039/c2dt30492a

The structural and dynamical aspects of alkylammonium salts of a silicodectungstate [(CH₃)₄N]₄[γ-SiW₁₀O₃₄(H₂O)₂] [C1], [(n-C₃H₇)₄N]₄[γ-SiW₁₀O₃₄(H₂O)₂] [C3], [(n-C₄H₉)₄N]₄[γ-SiW₁₀O₃₄(H₂O)₂] [C4], and [(n-C₅H₁₁)₄N]₄[γ-SiW₁₀O₃₄(H₂O)₂] [C5] were investigated. The results of sorption isotherms, XRD analyses, and solid-state NMR spectroscopy show that facile sorption of solvent molecules, flexibility of structures, and high mobility of alkylammonium cations are crucial to the uniform distribution of reactant and oxidant molecules throughout the bulk solid, which are related to the high catalytic activities for epoxidation of alkenes.

1. Introduction

H₂O₂-based catalytic epoxidation has received much attention from the economic and environmental viewpoints.^{1,2} Homogeneous transition metal catalysts such as titanium, iron, manganese, tungsten, and rhenium show high activities,^{1,2} and especially tungsten-based catalysts including polyoxometalates (POMs) show a high efficiency of H₂O₂ utilization and high selectivity to epoxides.^{1–7} However, most of these homogeneous systems share common drawbacks such as difficulty in catalyst/product separation and catalyst reuse. The immobilization of catalytically active species through ion exchange, adsorption, and covalent linkage can solve these drawbacks.^{8–12}

We have previously reported that a non-porous tetra-n-butylammonium salt of [γ-SiW₁₀O₃₄(H₂O)₂]⁴⁻, [(n-C₄H₉)₄N]₄[γ-SiW₁₀O₃₄(H₂O)₂]¹³ [C4], is an effective heterogeneous catalyst for size-selective epoxidation of alkenes with H₂O₂ in ethyl acetate (EtOAc).¹⁴ Various kinds of structurally diverse alkenes could efficiently be oxidized to the corresponding epoxides in high yields (Table 1).¹⁵ Non-activated C₃–C₆ terminal alkenes could efficiently be epoxidized. On the other hand, a longer reaction time was required for epoxidation of 1-octene to afford the corresponding epoxide in high yield, and the epoxide yield for larger 1-dodecene was much lower than those for C₃–C₈ terminal alkenes. Such size-selectivities were also

Table 1 Epoxidation of various alkenes with H₂O₂ catalyzed by C4^a

Entry	Alkene	Time [h]	Epoxide yield [%]
1 ^b	Propene	3	80
2 ^c	1-Butene	6	88
3	1-Hexene	5	92
4 ^d	1-Hexene	9	85
5 ^e	1-Hexene	5	75
6	<i>trans</i> -2-Hexene	12	80
7	<i>cis</i> -2-Hexene	2	92
8	1-Octene	19	90
9	1-Dodecene	27	17
10	Cyclopentene	1	95
11	Cyclohexene	2	81
12	Cyclooctene	3	>99
13	Cyclododecene	13	94

^a Reaction conditions: C4 (7.3 μmol), alkene (20 mmol), 60% H₂O₂ (1 mmol), EtOAc (6 mL), 333 K. Yield [%] = Epoxide [mol]/initial H₂O₂ × 100. ^b Propene (6 atm). ^c 1-Butene (2 atm). ^d 30% H₂O₂ (1 mmol). ^e C4 (14.6 μmol), 1-hexene (2 mmol), 60% H₂O₂ (1 mmol), EtOAc (2 mL), 333 K.

observed for epoxidation of C₅–C₁₂ cyclic alkenes. For epoxidation of *cis*- and *trans*-2-hexenes, the configurations around the C=C moieties were retained in the corresponding epoxides. Upon the sorption of EtOAc, the crystal system of C4 changes from tetragonal to cubic with an increase in the cell volume, and EtOAc molecules are highly mobile in the solid bulk of C4. The catalytic activity highly depends on the kinds of counter cations, while the effect of these counter cations on H₂O₂-based oxidation is still unclear.

Recently, it has become evident that the dynamics of catalyst structures and those of reactants and intermediates are related to the heterogeneous catalytic activity.^{16,17} For example, *in situ* scanning tunneling microscopy (STM) images revealed that the surface of metal-supported catalysts restructures during catalytic turnover as they bind, react, and release the adsorbed

Department of Applied Chemistry, School of Engineering, The University of Tokyo, 7-3-1 Hongo, Bunkyo-ku, Tokyo 113-8656, Japan. E-mail: imizuno@mail.ecc.u-tokyo.ac.jp; Fax: +81-3-5841-7220

† Electronic supplementary information (ESI) available: Powder XRD analyses of C3 (Fig. S1) and C5 (Fig. S2), space filling models of the crystal structure of alkylammonium salts (Fig. S3), powder XRD analyses of C3 (Fig. S4) and C5 (Fig. S5) immersed in EtOAc, intensities of the signals of ¹³C-CPMASNMR spectra as a function of contact times (Fig. S6–S10). See DOI: 10.1039/c2dt30492a

‡ Present Address: Department of Basic Sciences, School of Arts and Sciences, The University of Tokyo, 3-8-1 Komaba, Meguro-ku, Tokyo 153-8902, Japan.

molecules.^{16,17} The intermediates are also mobile and can quickly open active sites for continued catalytic turnovers.¹⁷ Similarly, solid-state NMR spectroscopy and quantum chemical calculations have shown that not only acidity but also mobility of protons has a large influence on heterogeneous acid catalysis of zeolites and heteropolyacids.^{18–20} The importance of dynamics in enzyme catalysts has been well known for years: The metal-containing active sites are surrounded by proteins with high conformational flexibility, which allow specific molecules to interact with the active sites contributing to the highly selective catalysis.^{21,22}

Based on these considerations, the structural and dynamical aspects of alkylammonium salts of a silicodecatungstate $[(\text{CH}_3)_4\text{N}]_4[\gamma\text{-SiW}_{10}\text{O}_{34}(\text{H}_2\text{O})_2]$ [**C1**], $[(n\text{-C}_3\text{H}_7)_4\text{N}]_4[\gamma\text{-SiW}_{10}\text{O}_{34}(\text{H}_2\text{O})_2]$ [**C3**], $[(n\text{-C}_4\text{H}_9)_4\text{N}]_4[\gamma\text{-SiW}_{10}\text{O}_{34}(\text{H}_2\text{O})_2]$ [**C4**], and $[(n\text{-C}_5\text{H}_{11})_4\text{N}]_4[\gamma\text{-SiW}_{10}\text{O}_{34}(\text{H}_2\text{O})_2]$ [**C5**] were investigated, and the results were related to their catalytic activities.²³

2. Experimental

Syntheses of alkylammonium salts of $[\gamma\text{-SiW}_{10}\text{O}_{34}(\text{H}_2\text{O})_2]^{4-}$ were carried out according to the literature procedure.^{13,14} The compounds were evacuated at 298–303 K before use and characterized by elemental analyses, IR spectroscopy, and thermogravimetry.

2.1. Catalytic epoxidation with H_2O_2

Epoxidation of propene and 1-hexene was carried out with an autoclave having a Teflon vessel and a 30 mL glass vessel, respectively. Catalytic epoxidation was carried out as follows: Catalyst (20 μmol for propene, 7.3 μmol for 1-hexene), propene (6 atm) or 1-hexene (20 mmol), EtOAc (6 mL) and 60% H_2O_2 (1 mmol) were charged in the reaction vessel. The reaction solution was heated at 333 K and was periodically analyzed by GC. The amount of remaining H_2O_2 was analyzed by $\text{Ce}^{3+/4+}$ titration. The conversion of H_2O_2 was almost 100%. Therefore, the yields were calculated based on initial H_2O_2 .

2.2. Powder X-ray diffraction study

Powder X-ray diffraction (XRD) patterns of **C1** and **C3–C5** as prepared and immersed in EtOAc were measured with an XRD-DSCII (Rigaku Corporation) and $\text{Cu K}\alpha$ radiation ($\lambda = 1.54056 \text{ \AA}$, 50 kV, 300 mA) at 303 K. The diffraction data were collected in the range of $2\theta = 4\text{--}25^\circ$ at 0.01° point and 5 s per step. The crystallographic parameters and the positions of the silicodecatungstate in **C3** and **C5** were calculated using Materials Studio Software (Accelrys Inc.) as follows: (i) the unit cell indexing and space group determination by X-cell,²⁴ (ii) peak profile fitting by the Pawley refinement,²⁵ (iii) structure optimization by the simulated annealing method,²⁶ and (iv) structure refinement by the Rietveld method.²⁷ The positions of the alkylammonium cations in **C3** and **C5** were optimized by molecular mechanics using universal force field (UFF),²⁸ since they could not be located with the powder XRD structure analysis because of the relatively low electron densities in the unit cell.

2.3. Vapor sorption measurement

EtOAc sorption isotherms of **C1** and **C3–C5** were measured at 298 K using an automatic volumetric vapor sorption apparatus Belsorp (BEL Japan Inc.). About 0.1 g of the compounds were evacuated at 298–303 K for >3 h to form the guest-free phases. Sorption equilibrium was judged by the following criteria: $\pm 0.3\%$ of pressure change in 5 min. Vapor saturation pressure (P_0) of EtOAc at 298 K was 12.9 kPa.

2.4. Solid-state ^{13}C cross polarization (CP) MAS NMR spectroscopy

NMR spectra were recorded at 298 K with a Chemagnetics CMX-300 Infinity spectrometer operating at 75.6 MHz for ^{13}C with MAS = 3 kHz and contact times of 0.01–100 ms. The spectrum of **C1** showed four signals at 57.2, 56.6, 56.0, and 55.3 ppm with the respective intensity ratio of ca. 1 : 1 : 1 : 1 for the **C1** carbons of $[(\text{CH}_3)_4\text{N}]^+$, probably because four $[(\text{CH}_3)_4\text{N}]^+$ per formula existed at crystallographically independent positions. The spectrum of **C3** showed three signals at 59.3, 16.1, and 11.3 ppm for **C1**, **C2**, and **C3** carbons of $[(n\text{-C}_3\text{H}_7)_4\text{N}]^+$, respectively. The spectrum of **C4** showed four signals at 57.9, 24.6, 20.3, and 14.9 ppm for **C1**, **C2**, **C3**, and **C4** carbons of $[(n\text{-C}_4\text{H}_9)_4\text{N}]^+$, respectively. The spectrum of **C5** showed four signals at 59.4, 28.6, 22.2, and 13.8 ppm for **C1**, **C3**, **C2** and **C4**, and **C5** carbons of $[(n\text{-C}_5\text{H}_{11})_4\text{N}]^+$, respectively.

3. Results and discussion

Table 2 summarizes effects of counter cations of **C1** and **C3–C5** epoxidation of alkenes with H_2O_2 . As previously reported, the catalytic activity using 1-hexene as a reactant changed in the order of **C1** (<1%) \ll **C3** (19%) < **C4** (92%) \approx **C5** (94%), and increased with the increase in the carbon chain lengths of the alkylammonium cations.¹⁴ The catalytic activity using the smaller propene increased in the same order of **C1** (6%) \ll **C3** (38%) < **C4** (89%) \approx **C5** (81%).

The crystal structures of **C1** and **C3–C5** are shown in Fig. 1. The crystal structures of **C1**¹³ and **C4**¹⁴ have been reported by single crystal X-ray diffraction analysis and powder X-ray diffraction analysis combined with molecular mechanics using UFF,²⁸ respectively. The crystal structures of **C3** and **C5** (Fig. S1 and S2†) were solved in the same way as that of **C4**. The

Table 2 Effect of counter cations on epoxidation of alkenes with H_2O_2 ^a

Catalyst	Epoxide yield [%]	
	Propene	1-Hexene ^b
C1	6	<1
C3	38	19
C4	89	92
C5	81	94

^a Reaction conditions: Catalyst 20 μmol , propene 6 atm, 60% H_2O_2 1 mmol, EtOAc 6 mL, 333 K, 300 min. Yield [%] = epoxide [mol]/initial H_2O_2 [mol] \times 100. ^b Data from ref. 14.

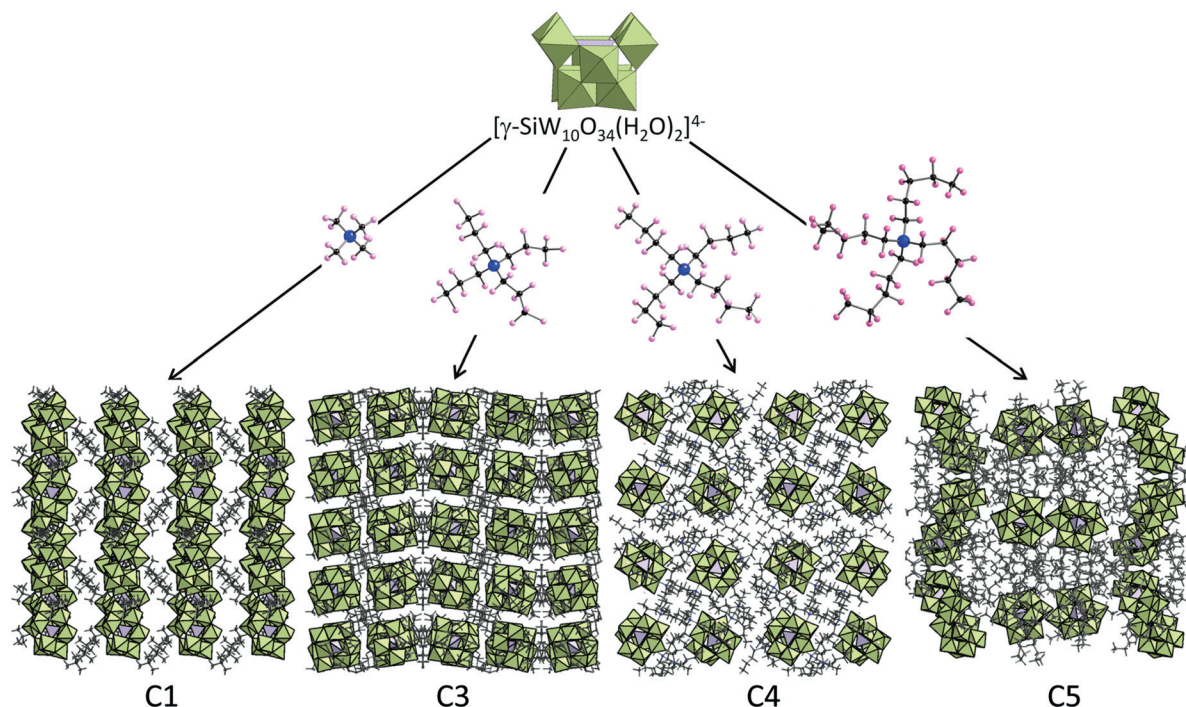


Fig. 1 Molecular structures of a silicodecatungstate and alkylammonium cations, and crystal structures of **C1** and **C3–C5**. Light green and purple polyhedra show the $[\text{WO}_6]$ and $[\text{SiO}_4]$ units, respectively. Black, blue, and pink spheres show the carbon, nitrogen, and hydrogen atoms of the alkylammonium cations, respectively.

silicodecatungstates in **C1** and **C3–C5** were packed into monoclinic, orthorhombic, tetragonal, and monoclinic cells, respectively. The alkylammonium cations of **C1** and **C3** were localized in the crystal lattice, while those of **C4** and **C5** were uniformly distributed in the crystal lattice. The space filling model of the structures (Fig. S3†) and N_2 adsorption isotherms (77 K) showed that all compounds were non-porous.

The EtOAc vapor sorption isotherms of the compounds at 298 K are shown in Fig. 2. Compounds **C4** and **C5** sorbed EtOAc from the low relative pressures, and the amounts at $P/P_0 = 0.8$ were *ca.* 1.5 mol mol^{-1} and were similar to each other. The amount of sorption by **C3** at $P/P_0 = 0.8$ was *ca.* 0.5 mol mol^{-1} and smaller than those of **C4** and **C5**. The amount of sorption by **C1** was *ca.* 0.1 mol mol^{-1} at $P/P_0 = 0.8$ and comparable to that of the surface adsorption. Thus, the amounts of EtOAc sorption increased in the order of **C1** \ll **C3** $<$ **C4** \approx **C5**, which was in line with the order of their catalytic activities and the hydrophobicity of alkylammonium cations (Table 2). As we have previously shown, both reactant (1-hexene) and oxidant (H_2O_2) were sorbed into the solid bulk of **C4** in the presence of EtOAc solvent.¹⁴ Therefore, the EtOAc sorption ability is crucial to the heterogeneous epoxidation catalyses of **C1** and **C3–C5**.

Compounds **C1** and **C3–C5** were immersed in EtOAc, and powder XRD patterns were measured to analyze the crystal structures (Fig. 3). Amounts of EtOAc sorption were estimated to be **C1** (0 mol mol^{-1}) \ll **C3** (*ca.* 0.5 mol mol^{-1}) $<$ **C4** \approx **C5** (*ca.* 1.0 mol mol^{-1}) with the ^{13}C NMR measurements. As we have previously shown, the powder XRD pattern of **C4** was changed by the immersion and the cell volume was increased by $\Delta V/Z = +156 \text{ \AA}^3$, which was comparable to the volume of the EtOAc molecule calculated with the molecular weight and

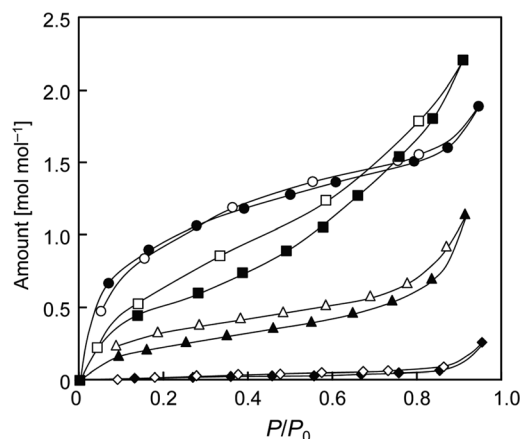


Fig. 2 EtOAc sorption–desorption isotherms of **C1** and **C3–C5**. Diamond, triangle, circle, and square symbols show the data for **C1** and **C3–C5**, respectively. Solid and open symbols show the sorption and desorption plots, respectively.

density of the liquid (162 \AA^3).¹⁴ The powder XRD pattern of **C5** also changed by the immersion and the cell volume was increased by $\Delta V/Z = +109 \text{ \AA}^3$ (Fig. S5†). On the other hand, the powder XRD pattern of **C3** changed little and the cell volume was increased only by $\Delta V/Z = +10 \text{ \AA}^3$ (Fig. S4†). These results show that **C4** and **C5** possess flexible structures while **C3** is rather rigid. According to Table 1, the catalytic activities of **C1** and **C3** for epoxidation of 1-hexene (yields of epoxides were $<1\%$ and 19% for **C1** and **C3**, respectively) were lower than those for epoxidation of the smaller propene (yields of epoxides in the presence of **C1** and **C3** were 6% and 38% , respectively).

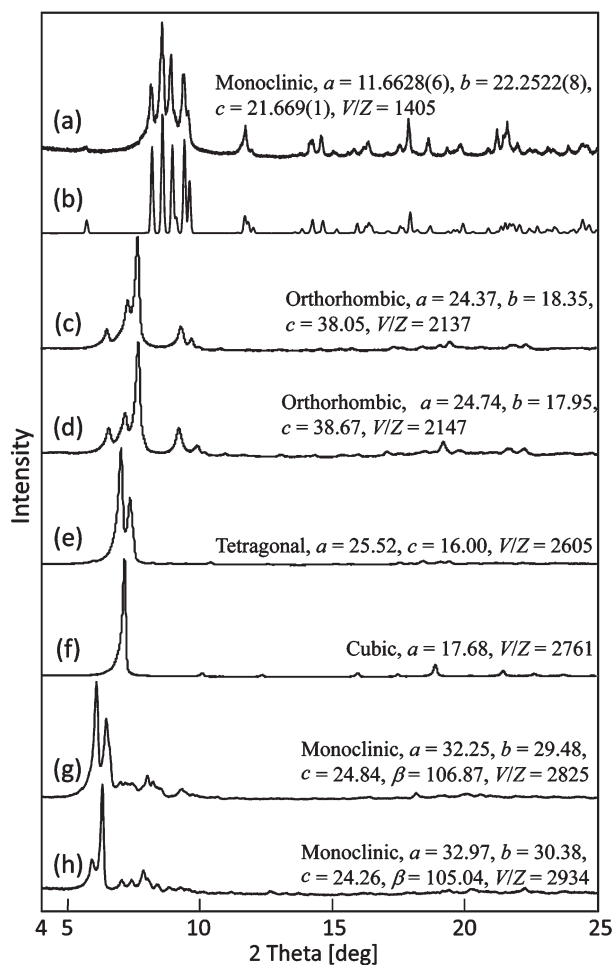


Fig. 3 Powder XRD patterns of **C1** and **C3–C5**. (a) **C1**, (b) calculated with the single crystal data of **C1**, (c) **C3**, (d) **C3** immersed in EtOAc, (e) **C4**, (f) **C4** immersed in EtOAc, (g) **C5**, and (h) **C5** immersed in EtOAc. Structural parameters were obtained by the Rietveld analysis²⁷ combined with molecular mechanics with UFF²⁸ except for **C1** (single crystal data).

The results of catalytic activities, sorption isotherms, and structural analyses, suggest that facile sorption of the solvent molecules (EtOAc) and structural flexibility of the catalysts are important factors, especially for epoxidation of larger alkenes.

The silicocatungstate is a rigid molecule since it is composed of covalent bonds of inorganic atoms, while the alkylammonium cations can be considered to be much more flexible since they are composed of single bonds between carbon, hydrogen, and nitrogen atoms. Thus, the flexibility of the alkylammonium cations may contribute to the structural flexibility of the catalysts. In order to investigate the flexibility (*i.e.*, mobility) of the alkylammonium cations, ¹³C CP (cross polarization) MASNMR spectroscopy was utilized. Fig. 4 shows the ¹³C CPMASNMR spectra of **C1** and **C3–C5** with different contact times (0.1, 0.5, 1.0, and 3.0 ms). The intensities of the signals increased with increase in contact times, reached a maximum, and then decreased. The relative intensity of the signals changed with the contact times: the relative intensity of the outer carbons increased with increasing contact time. The intensities of the signals were plotted against the contact time (Fig. S6–S10[†]), and

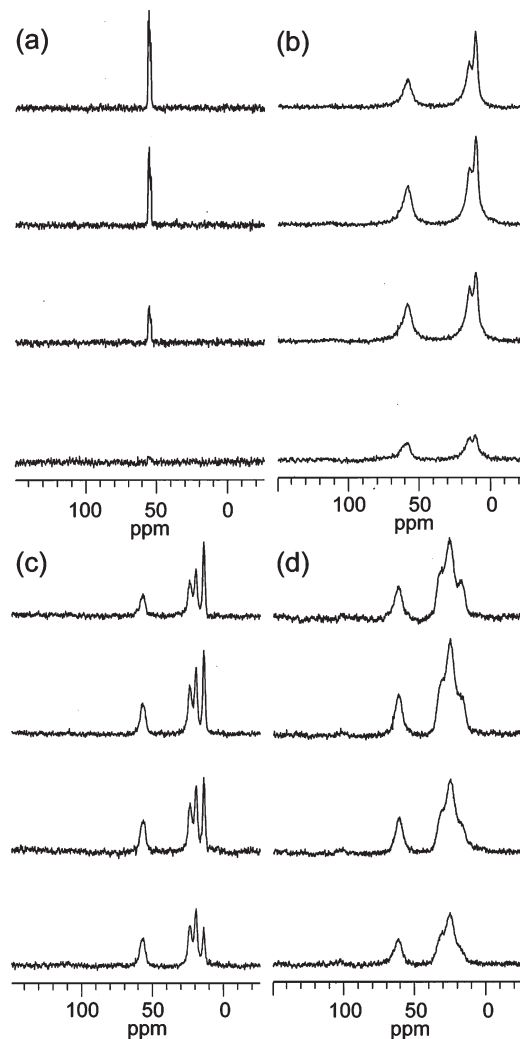


Fig. 4 Solid-state ¹³C CPMASNMR spectra of **C1** and **C3–C5**. (a) **C1**, (b) **C3**, (c) **C4**, and (d) **C5**. The cross polarization contact times from bottom to top were 0.1, 0.5, 1.0, and 3.0 ms.

the cross polarization time constant (T_{CH}) and proton spin-lattice relaxation time ($T_{1\rho(H)}$) were obtained for each carbon atom by using eqn (1), which describes the magnetization transfer from ¹H to ¹³C via the heteronuclear dipolar interactions:^{29,30}

$$I(t) = I_0(1 - T_{CH}/T_{1\rho(H)})^{-1} \{ \exp(-t/T_{1\rho(H)}) - \exp(-t/T_{CH}) \} \quad (1)$$

$I(t)$, I_0 , T_{CH} , and $T_{1\rho(H)}$ represent the intensity of the signal at contact time t , theoretical maximum intensity of the signal, cross polarization time constant, and proton spin-lattice relaxation time, respectively. The signal intensity of the less mobile carbon reaches a maximum at relatively short contact times (*i.e.*, shorter T_{CH}). The T_{CH} , and $T_{1\rho(H)}$ values are summarized in Table 3. The T_{CH} values increased from the inner carbon atoms to the outer carbon atoms suggesting that the outer carbon atoms are more mobile. The T_{CH} values of the most outer carbon atom increased in the order **C3** (C3 carbon: 0.54 ms) < **C4** (C4 carbon: 0.73 ms) < **C5** (C5 carbon: 1.5 ms), suggesting that the alkylammonium cations with longer carbon chains are more

Table 3 T_{CH} [ms] and T_{IP} [ms] values of the compounds

		Carbon in alkylammonium cation ^a				
		C1	C2	C3	C4	C5
C1	T_{CH}	9.1×10^{-1}	—	—	—	—
	T_{IP}	8.9	—	—	—	—
C3	T_{CH}	1.5×10^{-1}	2.8×10^{-1}	5.4×10^{-1}	—	—
	T_{IP}	4.0	4.2	5.5	—	—
C4	T_{CH}	7.5×10^{-2}	8.5×10^{-2}	1.7×10^{-1}	7.3×10^{-1}	—
	T_{IP}	6.3	5.5	5.5	5.1	—
C4-EtOAc	T_{CH}	5.5×10^{-2}	6.5×10^{-2}	1.5×10^{-1}	3.2×10^{-1}	—
	T_{IP}	1.5	2.1	1.4	2.4	—
C5	T_{CH}	3.5×10^{-1}	3.5×10^{-2}	3.5×10^{-1}	3.5×10^{-1}	1.5
	T_{IP}	5.8	7.5	8.7	7.5	12

^a Carbon atom which is adjacent to the nitrogen atom is denoted as C1.

mobile in the solid bulk. The T_{CH} values of $[(n\text{-C}_4\text{H}_9)_4\text{N}]^+$ in **C4** decreased with the sorption of EtOAc, suggesting that the highly mobile EtOAc molecules (T_{CH} : ca. 50 ms) interact with the alkylammonium cations and push their way through the solid bulk. While the mobility of $[(\text{CH}_3)_4\text{N}]^+$ in **C1** was relatively high (C1 carbon: 0.91 ms), **C1** could not sorb EtOAc so that reactants and oxidants could not enter and diffuse into the solid bulk for the catalytic reaction to occur there.

4. Conclusions

In conclusion, all these results show that facile sorption of solvent molecules (EtOAc), flexibility of the crystal structures of POM catalysts, and high mobility of alkylammonium cations are crucial to the uniform distribution of the reactant and oxidant molecules throughout the solid bulk of the catalyst and the high catalytic activity of heterogeneous catalysts of alkylammonium salts of a silicododecatungstate. These results suggest that not only the atomic structures of the active sites but also the structures and dynamics of the surroundings is important for the design and synthesis of highly active heterogeneous catalysts.

Acknowledgements

This work was supported in part by the Japan Society for the Promotion of Science (JSPS) through its Funding Program for World-Leading Innovative R&D on Science and Technology (FIRST Program), the Core Research for Evolutional Science and Technology (CREST) program of the Japan Science and Technology Agency (JST), Global COE Program (Chemistry Innovation through Cooperation of Science and Engineering), the Development in a New Interdisciplinary Field Based on Nanotechnology and Materials Science Programs, and

Grant-in-Aids for Scientific Research from the Ministry of Education, Culture, Science, Sports, and Technology of Japan.

Notes and references

- B. S. Lane and K. Burgess, *Chem. Rev.*, 2003, **103**, 2457–2473.
- S. T. Oyama, in *Mechanisms in Homogeneous and Heterogeneous Epoxidation Catalysis*, ed. S. T. Oyama, Elsevier, Amsterdam, 2008, pp. 1–99.
- R. Neumann, *Prog. Inorg. Chem.*, 1998, **47**, 317–370.
- I. V. Kozhevnikov, *Catalysts for Fine Chemical Synthesis: Catalysis by Polyoxometalates*, Wiley, Chichester, 2002.
- M. T. Pope, in *Comprehensive Coordination Chemistry II*, ed. J. A. McCleverty and T. J. Meyer, Elsevier Pergamon, Amsterdam, 2004, vol. 4, pp. 635–678.
- C. L. Hill, in *Comprehensive Coordination Chemistry II*, ed. J. A. McCleverty and T. J. Meyer, Elsevier Pergamon, Amsterdam, 2004, vol. 4, pp. 679–758.
- N. Mizuno, K. Kamata, S. Uchida and K. Yamaguchi, in *Modern Heterogeneous Oxidation Catalysis*, ed. N. Mizuno, Wiley-VCH, Weinheim, 2009, pp. 185–216.
- J. T. Rhule, W. A. Neiwert, K. I. Hardcastle, B. T. Do and C. L. Hill, *J. Am. Chem. Soc.*, 2001, **123**, 12101–12102.
- K. Yamaguchi, C. Yoshida, S. Uchida and N. Mizuno, *J. Am. Chem. Soc.*, 2005, **127**, 530–531.
- R. Neumann and H. Miller, *J. Chem. Soc., Chem. Commun.*, 1995, 2277–2278.
- B. Sels, D. De Vos, M. Buntinx, F. Pierard, A. Kirsch-DeMesmaeker and P. Jacobs, *Nature*, 1999, **400**, 855–857.
- K. Kamata, K. Yonehara, Y. Sumida, K. Hirata, S. Nojima and N. Mizuno, *Angew. Chem., Int. Ed.*, 2011, **50**, 12062–12066.
- K. Kamata, K. Yonehara, Y. Sumida, K. Yamaguchi, S. Hikichi and N. Mizuno, *Science*, 2003, **300**, 964–966.
- N. Mizuno, S. Uchida, K. Kamata, R. Ishimoto, S. Nojima, K. Yonehara and Y. Sumida, *Angew. Chem., Int. Ed.*, 2010, **49**, 9972–9976.
- While competitive epoxidation of various alkenes with different sizes has been reported,¹⁴ the substrate scope of **C4**-catalyzed epoxidation with H_2O_2 in EtOAc has not been investigated. Therefore, we extend the scope of the present catalytic system by carrying out epoxidation of $\text{C}_3\text{--C}_{12}$ terminal, internal, and cyclic alkenes with H_2O_2 (Table 1).
- G. A. Somorjai, A. M. Contreras, M. Montano and R. M. Rioux, *Proc. Natl. Acad. Sci. U. S. A.*, 2006, **103**, 10577–10583.
- P. L. Hansen, J. B. Wagner, S. Helveg, J. R. Rostrup-Nielsen, B. S. Clausen and H. Topsøe, *Science*, 2002, **295**, 2053–2055.
- M. Sierka and J. Sauer, *J. Phys. Chem. B*, 2001, **105**, 1603–1613.
- S. Uchida, K. Inumaru and M. Misono, *J. Phys. Chem. B*, 2000, **104**, 8108–8115.
- H. M. Kao and C. P. Grey, *J. Phys. Chem.*, 1996, **100**, 5105–5117.
- A. Fersht, *Structure and Mechanism in Protein Science: A Guide to Enzyme Catalysis and Protein Folding*, W. H. Freeman, New York, 1999.
- E. Z. Eisenmesser, D. A. Bosco, M. Akke and D. Kern, *Science*, 2002, **295**, 1520–1523.
- Since $[(n\text{-C}_6\text{H}_{13})_4\text{N}]_4[\gamma\text{-SiW}_{10}\text{O}_{34}(\text{H}_2\text{O})_2]$ [**C6**] was soluble in EtOAc, **C6** was not a heterogeneous catalyst.
- M. A. Neumann, *J. Appl. Crystallogr.*, 2003, **36**, 356–365.
- G. S. Pawley, *J. Appl. Crystallogr.*, 1981, **14**, 357–361.
- G. E. Engel, S. Wilke, O. König, K. D. M. Harris and F. J. J. Leusen, *J. Appl. Crystallogr.*, 1999, **32**, 1169–1179.
- H. M. Rietveld, *J. Appl. Crystallogr.*, 1969, **2**, 65–71.
- A. K. Rappé, C. J. Casewit, K. S. Colwell, W. A. Goddard III and W. M. Skiff, *J. Am. Chem. Soc.*, 1992, **114**, 10024–10035.
- C. A. Fyfe, A. C. Diaz, H. Grondy, A. R. Lewis and H. Förster, *J. Am. Chem. Soc.*, 2005, **127**, 7543–7558.
- S. H. C. Liang and I. D. Gay, *Langmuir*, 1985, **1**, 593–599.